Origin of High-T_C Ferromagnetism in Isovalent-Doped *III-V* Semiconductors

Peng Zhang,[1,2] Yong-Hyun Kim,[3] and Su-Huai Wei[2,4,*]

[1]*College of Physics and Optoelectronic Engineering, Shenzhen University, Shenzhen, Guangdong 518060, China*
[2]*Beijing Computational Science Research Center, Beijing 100094, China*
[3]*Graduate School of Nanoscience and Technology and Department of Physics, KAIST, Daejeon 305-701, Republic of Korea*
[4]*Beijing Advanced Innovation Center for Materials Genome Engineering, Beijing 100094, China*

(Received 5 February 2019; revised manuscript received 23 March 2019; published 22 May 2019)

Dilute magnetic semiconductors (DMSs) have attracted much attention because of their huge potential applications in spintronics. The simple band-coupling model suggests that isovalent doping of semiconductors (e.g., Mn-doped *II-V* semiconductors) should be antiferromagnetic due to the dominant superexchange interaction, which is consistent with experimental observations on most Mn-doped *II-VI* and Fe-doped *III-V* semiconductors (FDMSs). However, recently, it has been reported experimentally that some FDMSs are ferromagnetic with a very high Curie temperature (T_C) of over 300 K, but the underlying mechanism is not clear. Here, we reveal that the unusual ferromagnetism in FDMSs originates from a unique *p-d* coupling–induced band crossing and the resulting charge transfer from anion *p* to unoccupied Fe 3*d* orbitals. This result suggests that the ferromagnetism can be more easily realized by Fe doping in *III-V* semiconductors with high anion *p* orbital energies, such as GaSb, instead of those with small band gaps, such as InAs. Moreover, we illustrate that the isovalent character guarantees low self-compensation in FDMSs, which sets a major advantage to the realization of high T_C in FDMSs. Our finding can well explain the recent experimental observations and suggests a new avenue for the future design of high-T_C DMSs.

DOI: 10.1103/PhysRevApplied.11.054058

I. INTRODUCTION

Achieving high-Curie-temperature (T_C) ferromagnetism in conventional semiconductors has been a long-term dream for materials scientists, because of its potential application in spintronics [1]. At first glance, one may expect that this would be achieved naturally by doping the conventional semiconductors with magnetic impurities, such as transition metals. Dilute magnetic semiconductors (DMSs), born from this intuition, have attracted enormous attention over the past few decades [2–5]. The isovalent-doped DMSs (e.g., Mn-doped *II-VI* systems) were first considered, because the isovalent magnetic ions can be easily doped into the host semiconductors. Unfortunately, almost all the isovalent-doped DMSs were found to show antiferromagnetic (AFM) ground states. It was later realized that, when no carrier is introduced into the system, the superexchange interaction between the magnetic impurities dominates, which leads to antiferromagnetism [6]. On the other hand, with nonisovalent doping it is difficult to achieve a high solubility, which is required for high T_C. The pioneering work on high-concentration nonisovalent doping of Mn in InAs and GaAs through epitaxial growth by Ohno *et al.* [7–9] raised some hope to realize the dream again. However, after extensive studies of Mn-doped *III-V* semiconductors (MDMSs), it was realized that nonisovalent doping encounters doping limit issues, i.e., the formation of compensating defects, even though the low solubility could be overcome through nonequilibrium growth techniques [10]. These issues seriously limit the T_C of MDMSs, which, based on the Zener model [11,12], depends on both the magnetic impurity concentration (x) and the hole concentration (p), as $T_C \propto xp^{1/3}$. Therefore, it would be of great interest if one could find a system that could be doped as easily as isovalent-doped systems, but that could also introduce significant amounts of carriers into the system.

More recently, a new class of DMSs based on isovalent Fe-doped *III-V* semiconductors (FDMSs), such as $In_{1-x}Fe_xAs$ and $Ga_{1-x}Fe_xSb$, has been proposed [13–16]. It is interesting to see that an appreciable hole concentration (10^{18}–10^{19} cm^{-3}) can be injected into these FDMSs, which leads to robust ferromagnetic (FM) ground states. Moreover, the detrimental mechanism that limits T_C in MDMSs is not found in FDMSs. For example, in $Ga_{1-x}Fe_xSb$, it has been demonstrated experimentally that the carrier density increases monotonically with the defect concentration x [14], which provides a promising

*suhuaiwei@csrc.ac.cn

 © 2019 American Physical Society

way to realize high T_C in this system. Indeed, it has been reported that a relatively high T_C of over 300 K can be achieved in $Ga_{1-x}Fe_xSb$ at a defect concentration of $x = 25\%$ [15].

Despite these emerging merits, however, the fundamental mechanism that underlies the ferromagnetism in FDMSs is still not understood. Unlike MDMSs, where the ferromagnetism is hole-induced through nonisovalent doping, isovalent-doped FDMSs are usually expected to be AFM [6,17], apparently contradictory to experiments [13–15]. Moreover, the ferromagnetism in FDMSs is found to increase, as their hosts change from the wide-gap to narrow-gap semiconductors, e.g., from $Ga_{1-x}Fe_xAs$ to $Ga_{1-x}Fe_xSb$ [14,18], in sharp contrast to what has been found in MDMSs, where the ferromagnetism decreases from $Ga_{1-x}Mn_xAs$ to $Ga_{1-x}Mn_xSb$ [6,17,19]. Furthermore, it has been shown experimentally that $In_{1-x}Fe_xAs$ behaves like n-type electron-induced DMSs, whereas $Ga_{1-x}Fe_xSb$ shows p-type hole-induced DMSs [13–16]. This bipolar-doping behavior is often speculated to be ascribed to the formation of different native defects in these materials. However, this speculation does not explain why the hole concentration in $Ga_{1-x}Fe_xSb$ is found to increase with x [14], provided that holes are generated by the native defects. Although the electron-induced ferromagnetism has been demonstrated in $In_{1-x}Fe_xAs$ by co-doping with nonmagnetic donors [13,16], it is still an open question whether the ferromagnetism in intrinsic FDMSs is electron- or hole-induced.

To clarify these ambiguities and to unravel the origin of the ferromagnetism in isovalent-doped FDMSs, in this article we systematically study the electronic structures and magnetic properties of several prototype FDMSs, including $Ga_{1-x}Fe_xAs$, $Ga_{1-x}Fe_xSb$, $In_{1-x}Fe_xAs$, and $In_{1-x}Fe_xSb$, by using first-principles calculations and orbital analysis. Our results indicate that the ferromagnetism can be stabilized in $Ga_{1-x}Fe_xSb$ and $In_{1-x}Fe_xSb$, which has high valence-band (VB) energies, but not in $Ga_{1-x}Fe_xAs$ and $In_{1-x}Fe_xAs$, where AFM states are more stable, even though InAs has a much smaller band gap than GaSb. Based on the band-coupling model, we find that the ferromagnetism in Sb compounds originates from a unique p-d coupling–induced band crossing and the resulting charge transfer from Sb $5p$ to Fe $3d$ orbitals, which is thus hole-mediated. This result indicates that it is the VB energies, rather than the band gaps, of the host semiconductors that determine the magnetic ground states in FDMSs. Moreover, our calculations also reveal that, unlike Mn interstitials (Mn_i) in $Ga_{1-x}Mn_xAs$, the Fe interstitials (Fe_i) cannot be easily formed in $Ga_{1-x}Fe_xSb$, because of their higher valence state, which leads to a higher formation energy than that of substitutional isovalent Fe impurities (Fe_{Ga}). This explains the experimentally observed monotonic relationship between the carrier density and defect concentration in FMDSs.

II. COMPUTATIONAL METHODS

Our calculations are carried out by using the projector augmented wave (PAW) method [20] and the Heyd-Scuseria-Ernzerhof (HSE06) hybrid functional [21] within the density-functional theory (DFT) as implemented in VASP [22]. A cutoff energy of 400 eV is used for the plane-wave basis set, and a Γ-centered $4 \times 4 \times 4$ Monkhorst–Pack k-mesh is used for the Brillouin-zone integration. For all the calculations, the atomic positions are relaxed until the Hellman-Feynman force on each atom is less than 0.01 eV/Å.

For defect calculations, we use a $2 \times 2 \times 2$ supercell of the zincblende structure that contains a single defect. For a defect α in the charge state q, its formation energy $(\Delta H_f(\alpha,q))$ is calculated by [23,24]

$$\Delta H_f(\alpha, q) = \Delta E(\alpha, q) + \sum n_i\mu_i + qE_F, \quad (1)$$

where $\Delta E(\alpha, q) = E(\alpha, q) - E(\text{host}) + \sum n_i E_i + q\varepsilon_{\text{VBM}}$ (host). Here, $E(\text{host})$ is the total energy of the supercell containing 64 atoms and $E(\alpha, q)$ is the total energy of the same supercell but with a defect α. The Fermi level (E_F) is referenced to the VBM of the host, μ_i is the chemical potential of constituent element i referenced to elemental solid with energy E_i, n_i is the number of elements, and q is the number of electrons transferred from the supercell to reservoirs in forming the defect cell. Here μ_i is restricted by several thermodynamic conditions. Firstly, precipitation of the elemental dopant and host elements is avoided. For example, for $Ga_{1-x}Fe_xSb$, μ_i is limited by

$$\mu_{\text{Ga}} \le \mu(\text{Ga bulk}) = 0, \quad (2)$$

$$\mu_{\text{Sb}} \le \mu(\text{Sb bulk}) = 0, \quad (3)$$

$$\mu_{\text{Fe}} \le \mu(\text{Fe bulk}) = 0. \quad (4)$$

Here, the μ (Ga bulk) is calculated by the orthorhombic structure (space group $Cmca$) of bulk Ga, μ (Sb bulk) is calculated by the trigonal structure (space group $R\bar{3}m$) of bulk Sb, and μ (Fe bulk) is calculated by the cubic structure (space group $Fm\bar{3}m$) of bulk Fe.

Secondly, μ_{Ga} and μ_{Sb} are limited to the values for maintaining stable GaSb. Therefore,

$$\mu_{\text{Ga}} + \mu_{\text{Sb}} = \Delta H_f(\text{GaSb}), \quad (5)$$

where $\Delta H_f(\text{GaSb})$ is the formation energy of bulk GaSb (zincblende structure, space group $F\bar{4}3m$). Third, to avoid the formation of the possible secondary phases, e.g., $FeSb_2$, μ_{Fe} is also limited by

$$\mu_{\text{Fe}} + 2\mu_{\text{Sb}} \le \Delta H_f(\text{FeSb}_2), \quad (6)$$

where $\Delta H_f(\text{FeSb}_2)$ is the formation energy of bulk $FeSb_2$. With all these restrictions considered, the stable chemical

potential range of $Ga_{1-x}Fe_xSb$ can then be obtained (more details and stable chemical potential ranges of $Ga_{1-x}Fe_xSb$ and $Ga_{1-x}Mn_xAs$ are given in the Supplemental Material [25]).

III. RESULTS AND DISCUSSIONS

III-V semiconductors have a typical zincblende structure with T_d symmetry. The valence-band maximum (VBM) of these semiconductors is composed mainly of anion p orbitals, as well as some cation p and d orbitals, forming the triply degenerate t_{2p} states, while the conduction-band minimum (CBM) consists mainly of cation s orbitals, mixed with some anion s orbitals, forming the a_{1s} state (see Fig. S1 in the Supplemental Material [25]). The calculated band gaps of the four studied host semiconductors are given in Table I, along with the experimental data. To overcome the well-known local density approximation or generalized gradient approximation error, the hybrid functional (HSE06) is employed. The calculated band gaps are in good agreement with experiments, with the largest deviation of approximately 0.22 eV for GaAs, which is consistent with previous calculations [27]. This result indicates that our calculations can well capture the electronic structures of the host semiconductors and give us confidence for further investigating the electronic and magnetic properties of the corresponding FDMSs.

To estimate the stability of ferromagnetism in FDMSs, we next calculate the FM stabilization energy ($\Delta E_{\text{FM-AFM}}$), which is defined by the energy difference between the FM and AFM phases. Here, we adopt the nearest-neighbor (NN) configuration, where the two host cations (Ga or In) as the first face-centered-cubic (fcc) neighbors are replaced by a pair of Fe atoms in a $2 \times 2 \times 2$ supercell of the zincblende structure that contains 64 atoms (see Fig. S2 in the Supplemental Material [25]). The FM or AFM phases are then established by aligning the spin orientations of the two Fe atoms parallel or antiparallel to each other. The calculated $\Delta E_{\text{FM-AFM}}$ and magnetic ground states for FDMSs are given in Table I. From these calculations, two main conclusions are obtained:

TABLE I. Calculated host band gaps and energy difference ($\Delta E_{\text{FM-AFM}}$) between the FM and AFM phases for Fe-doped semiconductors. The experimental band gaps are also given in parentheses for comparison.

System	Host band gap (eV)	$\Delta E_{\text{FM-AFM}}$ (meV)	Ground state
$Ga_{1-x}Fe_xAs$	1.30 (1.52[a])	346	AFM
$Ga_{1-x}Fe_xSb$	0.91 (0.82[a])	−108	FM
$In_{1-x}Fe_xAs$	0.30 (0.42[a])	104	AFM
$In_{1-x}Fe_xSb$	0.22 (0.24[a])	−80	FM

[a]Ref. [26].

(i) It is clear to see that the ferromagnetism can be stabilized in some FDMSs, despite the substitutional Fe atoms being isovalent to the host cations. We find that, among the four studied FDMSs, $Ga_{1-x}Fe_xAs$ favors the AFM ground state, while $Ga_{1-x}Fe_xSb$ and $In_{1-x}Fe_xSb$ favor the FM ground states, which is consistent with experiments [14,18]. For $In_{1-x}Fe_xAs$, it should be noted that although the electron-induced ferromagnetism has been realized by co-doping with nonmagnetic donors [13,16], our calculations show that the intrinsic $In_{1-x}Fe_xAs$ possesses the AFM ground state with a positive $\Delta E_{\text{FM-AFM}} =$ 104 meV.

(ii) The magnetic ground states of FDMSs do not depend on the band gaps, but on the valence-band (VB) energies of their host semiconductors, which mainly depend on the anion p orbital energies. We see that the calculated band gaps decrease from GaAs to GaSb to InAs and to InSb. However, the change of $\Delta E_{\text{FM-AFM}}$ for the corresponding FDMSs deviates obviously from this trend. It is found that the As compounds generally possess the AFM ground states, while the Sb compounds possess the FM ground states, implying a close relationship between the magnetic properties of these materials and their host anions. This is quite different from what has been observed in MDMSs, where the FM stability typically increases with the host band gaps [6,17,19,28].

To further understand these results, we calculate the total density of states (DOS) and Fe 3d projected density of states (PDOS) of FDMSs in both the AFM and FM phases, as shown in Fig. 1. For all these systems, we find that their VBMs are constructed mainly by the anion t_{2p} states, similar to their host semiconductors. The 3d orbitals of the substitutional Fe atoms show a large exchange splitting between the majority and minority states. Under the tetrahedral crystal filed, these Fe 3d orbitals split into the triply degenerate t_{2d} and doubly degenerate e_d states. The Fe t_{2d} states can then couple with the anion t_{2p} states in the same spin configuration. As a result, for the FM phases of FDMSs, an energy splitting between the majority and minority channels can be generally observed, especially for the states near the Fermi level (FL), as shown in Figs. 1(a)–1(d). For $Ga_{1-x}Fe_xAs$ and $In_{1-x}Fe_xAs$, we find that both the AFM and FM phases are semiconductors, which is consistent with the usual expectation for isovalent doping. However, for $Ga_{1-x}Fe_xSb$ and $In_{1-x}Fe_xSb$, it is surprising to see that, although the AFM phases are also semiconductors, the FM phases become metallic with the FL crossing the VB within the majority channel. According to the band-coupling model [6,17], the holes introduced into the VB are essential to stabilize the FM phase of the system. For example, it has been demonstrated that the metallic $Ga_{1-x}Mn_xAs$ favors the FM ground state, while the semiconducting $Cd_{1-x}Mn_xTe$ favors the AFM ground state [6]. The metallicity may explain why $Ga_{1-x}Fe_xSb$

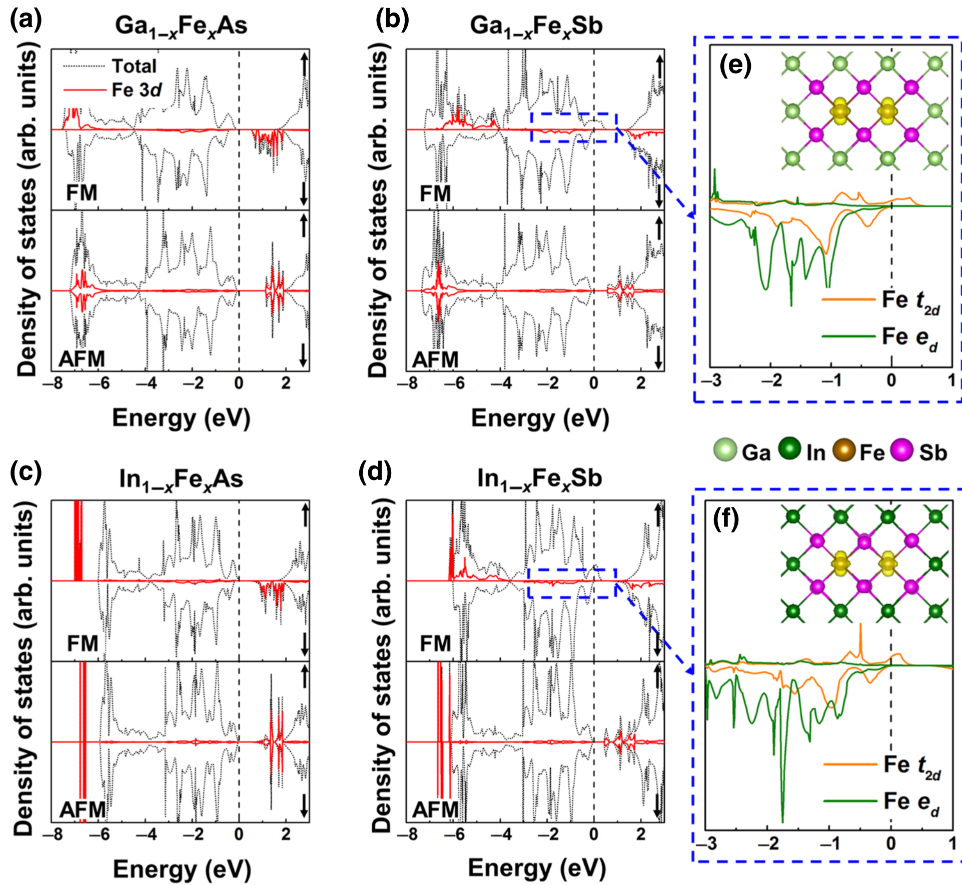

FIG. 1. Calculated total (DOS) and Fe 3d projected density of states (PDOS) for (a) Ga$_{1-x}$Fe$_x$As, (b) Ga$_{1-x}$Fe$_x$Sb, (c) In$_{1-x}$Fe$_x$As, and (d) In$_{1-x}$Fe$_x$Sb. The Fe t_{2d} and e_d PDOSs are within the energy range between −3 and 1 eV. The corresponding local charge density for (e) Ga$_{1-x}$Fe$_x$Sb and (f) In$_{1-x}$Fe$_x$Sb. The majority and minority spin channels are labeled by the upward and downward arrows, respectively. The isosurface of charge density is selected to be 0.04 e/Å^3.

and In$_{1-x}$Fe$_x$Sb have the FM ground states. However, one important question is where do the holes in the VB come from, because different from MDMSs, one may expect that the isovalent substitution of host cations by Fe atoms is unlikely to introduce holes, similar to the case of Mn-doped *II-VI* semiconductors.

To answer this question and get more insight into the ferromagnetism in FDMSs, we employ the band-coupling model to further analyze the band structures of these materials, as shown in Fig. 2(a). Here, we only discuss the energy levels near the FL, which play the major role (the detailed band-coupling model is given in Fig. S3 in the Supplemental Material [25]). As shown in Fig. 2(a), when two cations in the host semiconductors are substituted by a pair of Fe atoms, the interaction between anion t_{2p} (also with some Fe t_{2d} component) dominated states and that between Fe e_d states at the substituted sites could occur, generating the bonding ($t^{b}_{2p\uparrow}$ or $e^{b}_{d\downarrow}$) and antibonding ($t^{ab}_{2p\uparrow}$ or $e^{ab}_{d\downarrow}$) states. For FDMSs, depending on the relative energy of Fe e_d versus host t_{2p} states, two different cases could occur:

(i) If the t_{2p} states lie well below the Fe e_d states and the p-p (d-d) coupling between t_{2p} (e_d) states is weak, the $t^{ab}_{2p\uparrow}$ states would have a lower energy than the $e^{b}_{d\downarrow}$ states, as shown in the left panel of Fig. 2(a). In this case, the $t^{ab}_{2p\uparrow}$ states are fully occupied while the $e^{b}_{d\downarrow}$ states are fully empty, making the materials semiconductors. This is similar to what has been found in Mn-doped *II-VI* semiconductors [6]. It is clear to see that no energy gain can be obtained by the FM coupling between the t_{2p} (or the e_d) states and thus the system prefers the AFM ground state.

(ii) If the anion t_{2p} states lie close to the Fe e_d states and the p-p (d-d) coupling between the t_{2p} (e_d) states is strong, the $e^{b}_{d\downarrow}$ states would be pushed down to below the $t^{ab}_{2p\uparrow}$ states, leading to a p-d band crossing, as illustrated in the right panel of Fig. 2(a). In this case, electrons originally occupying the $t^{ab}_{2p\uparrow}$ states will fall into the $e^{b}_{d\downarrow}$ states, leaving the $t^{ab}_{2p\uparrow}$ states partially occupied. As can be seen from Fig. 2(b), the charge transfer from $t^{ab}_{2p\uparrow}$ to $e^{b}_{d\downarrow}$ states would gain energy. Consequently, when the FM coupling overwhelms the AFM coupling, FM will become the ground state of the system. This is the usual case because,

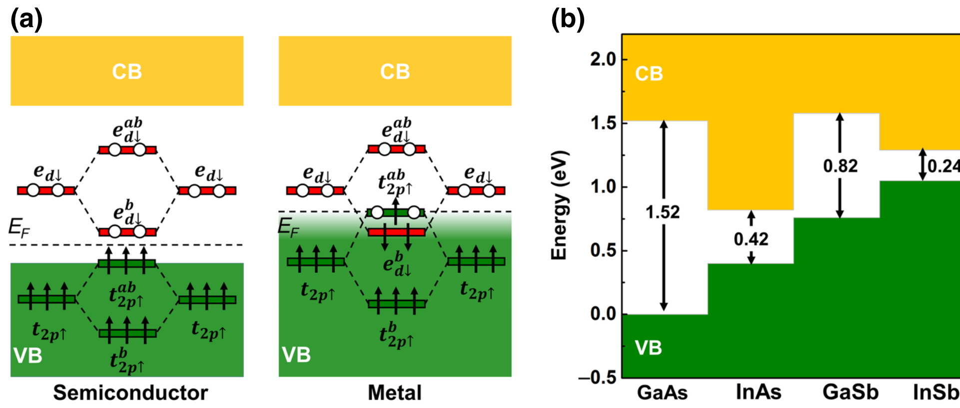

FIG. 2. (a) Schematic band-coupling model for antiferromagnetic and ferromagnetic ground states for FMDSs. (b) Calculated valence-band alignment between GaAs, InAs, GaSb, and InSb. The band edge is referenced to the VBM of GaAs. The experimental band gaps are used to align the conduction-band edges.

due to the perturbation theory of quantum mechanics, the coupling strength is inversely dependent on the energy separation. For the FM configuration, the coupling states are nearly degenerate, whereas in the AFM configuration, the coupling states are separated by the exchange splitting, so that the FM coupling is usually much larger than the AFM coupling.

For $Ga_{1-x}Fe_xAs$ and $In_{1-x}Fe_xAs$, the VBM is composed mainly of As $4p$ orbitals that have much lower energy than the Fe e_d states. Thus, the p-d coupling–induced band crossing cannot occur and the compounds are semiconductors with the AFM ground states, as shown in Figs. 1(a) and 1(c). However, for $Ga_{1-x}Fe_xSb$ and $In_{1-x}Fe_xSb$, the VBM is derived from the Sb $5p$ orbitals that have much higher energy than As $4p$ orbitals. Consequently, the p-d band crossing and thus the charge transfer from $t_{2p\uparrow}^{ab}$ to $e_{d\downarrow}^{b}$ states occurs, which renders these compounds to be metallic and possess the FM ground states, as shown in Figs. 1(b) and 1(d). These results imply that the ferromagnetism in FDMSs is closely related to the VB energies of their host semiconductors, not simply the band gaps as previously suggested [11]. Fig. 2(b) plots the calculated band alignments for the four studied host semiconductors. The VB edge energies are consistent with our previous calculations [26] and show a good agreement with experiments. For example, the GaAs/InAs offset is calculated to be 0.50 eV, in good agreement with deep-level transient spectroscopy measurements of 0.46 eV [29]. The experimental band gaps [30] are then used to position the conduction-band (CB) edges. It can be seen that the VBMs of Sb compounds are roughly 0.75 eV higher than the corresponding As compounds, suggesting that the p-d band crossing can occur more easily in Sb compounds than in As compounds. To identify the character of the occupied Fe $3d$ states, we plot the local charge density for the PDOS of $Ga_{1-x}Fe_xSb$ and $In_{1-x}Fe_xSb$ from -3 to 0 eV below the FL, as show in Figs. 1(e) and 1(f). It is clear to see that the occupied Fe $3d$ orbitals within the minority channel have a predominate e_d character, which is consistent with our band-coupling model.

In the above discussion, we assume the fcc NN configuration for the substitutional Fe pairs. In reality, the Fe-Fe separation could be larger. To check the validity of our band-coupling model in DMSs, we have considered another configuration with the largest Fe-Fe distance (LD) in a 64-atom supercell of $Ga_{1-x}Fe_xSb$ (see Fig. S2 in the Supplemental Material [25]). Table II gives the calculated total energies for the FM and AFM phases, as well as their energy differences, of $Ga_{1-x}Fe_xSb$ with both the NN and LD configurations. It is interesting to see that the stabilization energy of the FM phase in the LD configuration changes slowly with Fe-Fe distance and could even be enhanced, compared to the NN configuration. This can be ascribed to the fact that, as the Fe-Fe distance increases, both the FM and AFM couplings decrease, but the latter changes more rapidly than the former, due to the more localized orbitals. These results, therefore, suggest that the availability of the band-coupling model can be general in DMSs.

It is well known that the defect property of DMSs has a significant impact on their electronic and magnetic performances. For example, in MDMSs, one major challenge to realize high T_C is the spontaneous formation of compensating defects, such as Mn_i, when the materials are

TABLE II. Calculated total energies for the FM and AFM states, as well as their differences, of $Ga_{1-x}Fe_xSb$ with both the NN and LD configurations.

Configuration	E_{FM} (eV)	E_{AFM} (eV)	$\Delta E_{FM\text{-}AFM}$ (meV)
NN	−302.004	−301.896	−108
LD	−301.959	−301.789	−170

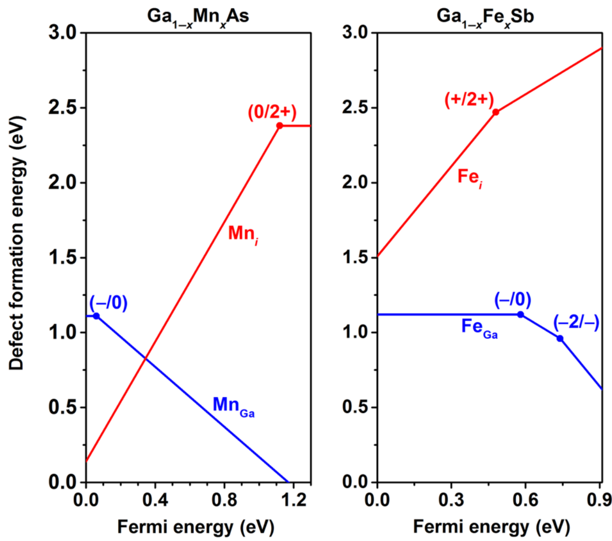

FIG. 3. Calculated formation energies for interstitial and substitutional Mn impurities in $Ga_{1-x}Mn_xAs$ and interstitial and substitutional Fe impurities in $Ga_{1-x}Fe_xSb$ under the Mn-rich and Fe-rich conditions (point T in Fig. S1 in the Supplemental Material [25]).

heavily doped, which limits the achievable carrier density [31–34]. However, in FDMSs, the carrier density is found to increase monotonically with the defect concentration, which is a promising feature that can be used to realize high T_C [14,15]. To understand these experimental observations, we calculate the defect formation energies for Fe_{Ga} and Fe_i in $Ga_{1-x}Fe_xSb$, and compare them with that for Mn_{Ga} and Mn_i in $Ga_{1-x}Mn_xAs$, as illustrated in Fig. 3. It is clear to see that the calculated formation energy of Fe_{Ga} in $Ga_{1-x}Fe_xSb$ is similar to that of Mn_{Ga} in $Ga_{1-x}Mn_xAs$, which indicates that Fe_{Ga} in $Ga_{1-x}Fe_xSb$ should have a similar solubility to Mn_{Ga} in $Ga_{1-x}Mn_xAs$. Thus, to achieve a high doping concentration, a nonequilibrium growth method, such as molecular beam epitaxy (MBE), must be used for both of these systems [10,14]. Moreover, we find that for $Ga_{1-x}Mn_xAs$, Mn_i tends to be energetically more favorable than Mn_{Ga}, when x increases and the FL approaches the VBM. The formation of Mn_i, as a donor, would compensate for the holes induced by Mn_{Ga} and thus significantly reduce the carrier density and T_C of the system. This is consistent with the experimental observations that T_C of $Ga_{1-x}Mn_xAs$ cannot exceed room temperature, even for a large defect concentration of $x = 20\%$ [10]. For $Ga_{1-x}Fe_xSb$, on the other hand, the formation energy of Fe_i remains larger than that of Fe_{Ga} across the whole Fermi energy range between VBM and CBM, because Fe has more valence charges, which indicates that the Fe_i cannot form easily even at high Fe_{Ga} concentrations. This characteristic resistance of the formation of hole killers explains why the hole density can increase monotonically with x in $Ga_{1-x}Fe_xSb$ [14,15], which implies that there is a great potential to realize high T_C in isovalent-doped FDMSs.

IV. CONCLUSION

Based on first-principles calculations, we systematically study the electronic and magnetic properties of several prototype isovalent FDMSs. We find that $Ga_{1-x}Fe_xAs$ and $In_{1-x}Fe_xAs$ favor the AFM ground states, while $Ga_{1-x}Fe_xSb$ and $In_{1-x}Fe_xSb$ favor the FM ground states. More importantly, our calculations show that the ferromagnetism in Sb compounds originates from a unique p-d band crossing and the resulting charge transfer from Sb $5p$ to Fe $3d$ orbitals, and thus is hole-mediated. Accordingly, we show that it is the VB energies, rather than the band gaps of the host semiconductors, that essentially influence the magnetic ground state in FDMSs. This mechanism is quite different from the previous understanding obtained in MDMSs. Moreover, we identify a major advantage of isovalent-doped FDMSs over nonisovalent-doped MDMDs, i.e., the resistance of the formation of compensating defects, such as Fe_i, which may result in a relatively high carrier concentration and thus high T_C. Our findings, therefore, significantly broaden the recent understanding of the magnetic behaviors in DMSs and suggest an alternative strategy for the future design of high-T_C DMSs for spintronics.

ACKNOWLEDGMENTS

This work was supported by the Science Challenge Project, under Grant No. TZ2016003, the National Key Research and Development Program of China (Grant No. 2016YFB0700700), and the National Nature Science Foundation of China (Grants No. 51672023, No. 11634003, No. U1530401, No. 61827815, and No. 11774239). Y.-H.K. was supported by the National Research Foundation of Korea (Grants No. 2015R1A2A2 A05027766 and No. 2016R1A5A1008184). The computation was supported by the Beijing Computational Science Research Center (CSRC). We also acknowledge Jianhua Zhao and Hailong Wang for their discussions and constructive suggestions.

[1] S. Wolf, D. Awschalom, R. Buhrman, J. Daughton, S. Von Molnar, M. Roukes, A. Y. Chtchelkanova, and D. Treger, Spintronics: A spin-based electronics vision for the future, Science **294**, 1488 (2001).

[2] T. Dietl, A ten-year perspective on dilute magnetic semiconductors and oxides, Nat. Mater. **9**, 965 (2010).

[3] K. Sato, L. Bergqvist, J. Kudrnovský, P. H. Dederichs, O. Eriksson, I. Turek, B. Sanyal, G. Bouzerar, H. Katayama-Yoshida, V. A. Dinh, T. Fukushima, H. Kizaki, and R. Zeller, First-principles theory of dilute magnetic semiconductors, Rev. Mod. Phys. **82**, 1633 (2010).

[4] T. Dietl and H. Ohno, Dilute ferromagnetic semiconductors: Physics and spintronic structures, Rev. Mod. Phys. **86**, 187 (2014).

[5] T. Dietl, K. Sato, T. Fukushima, A. Bonanni, M. Jamet, A. Barski, S. Kuroda, M. Tanaka, P. N. Hai, and H. Katayama-Yoshida, Spinodal nanodecomposition in semiconductors doped with transition metals, Rev. Mod. Phys. **87**, 1311 (2015).

[6] G. M. Dalpian, S.-H. Wei, X. G. Gong, A. J. R. da Silva, and A. Fazzio, Phenomenological band structure model of magnetic coupling in semiconductors, Solid State Commun. **138**, 353 (2006).

[7] H. Munekata, H. Ohno, S. von Molnar, A. Segmuller, L. L. Chang, and L. Esaki, Diluted Magnetic III-V Semiconductors, Phys. Rev. Lett. **63**, 1849 (1989).

[8] H. Ohno, H. Munekata, T. Penney, S. Von Molnar, and L. Chang, Magnetotransport Properties of p-Type (In, Mn) As Diluted Magnetic III-V Semiconductors, Phys. Rev. Lett. **68**, 2664 (1992).

[9] H. Ohno, A. Shen, F. Matsukura, A. Oiwa, A. Endo, S. Katsumoto, and Y. Iye, (Ga, Mn)As: A new diluted magnetic semiconductor based on GaAs, Appl. Phys. Lett. **69**, 363 (1996).

[10] L. Chen, X. Yang, F. Yang, J. Zhao, J. Misuraca, P. Xiong, and S. von Molnár, Enhancing the Curie temperature of ferromagnetic semiconductor (Ga, Mn) As to 200 K via nanostructure engineering, Nano Lett. **11**, 2584 (2011).

[11] T. Dietl, H. Ohno, F. Matsukura, J. Cibert, and E. D. Ferrand, Zener model description of ferromagnetism in zinc-blende magnetic semiconductors, Science **287**, 1019 (2000).

[12] T. Dietl, H. Ohno, and F. Matsukura, Hole-mediated ferromagnetism in tetrahedrally coordinated semiconductors, Phys. Rev. B **63**, 195205 (2001).

[13] P. Nam Hai, L. Duc Anh, S. Mohan, T. Tamegai, M. Kodzuka, T. Ohkubo, K. Hono, and M. Tanaka, Growth and characterization of n-type electron-induced ferromagnetic semiconductor (In, Fe)As, Appl. Phys. Lett. **101**, 182403 (2012).

[14] N. T. Tu, P. N. Hai, L. D. Anh, and M. Tanaka, (Ga, Fe)Sb: A p-type ferromagnetic semiconductor, Appl. Phys. Lett. **105**, 132402 (2014).

[15] N. T. Tu, P. N. Hai, L. D. Anh, and M. Tanaka, High-temperature ferromagnetism in heavily Fe-doped ferromagnetic semiconductor (Ga, Fe)Sb, Appl. Phys. Lett. **108**, 192401 (2016).

[16] L. D. Anh, P. N. Hai, and M. Tanaka, Observation of spontaneous spin-splitting in the band structure of an n-type zinc-blende ferromagnetic semiconductor, Nat. Commun. **7**, 13810 (2016).

[17] H. Peng, J. Li, and S.-H. Wei, Chemical trends of magnetic interaction in Mn-doped III-V semiconductors, Appl. Phys. Lett. **102**, 2013 (2013).

[18] S. Haneda, M. Yamaura, Y. Takatani, K. Hara, S.-I. Harigae, and H. Munekata, Preparation and characterization of Fe-based III-V diluted magnetic semiconductor (Ga, Fe) As, Jpn. J. Appl. Phys. **39**, L9 (2000).

[19] P. Mahadevan and A. Zunger, Trends in ferromagnetism, hole localization, and acceptor level depth for Mn substitution in GaN, GaP, GaAs, and GaSb, Appl. Phys. Lett. **85**, 2860 (2004).

[20] G. Kresse and D. Joubert, From ultrasoft pseudopotentials to the projector augmented-wave method, Phys. Rev. B **59**, 1758 (1999).

[21] J. Heyd, G. E. Scuseria, and M. Ernzerhof, Hybrid functionals based on a screened Coulomb potential, J. Chem. Phys. **118**, 8207 (2003).

[22] G. Kresse and J. Furthmüller, Efficiency of ab-initio total energy calculations for metals and semiconductors using a plane-wave basis set, Comput. Mater. Sci. **6**, 15 (1996).

[23] S.-H. Wei and S. B. Zhang, Chemical trends of defect formation and doping limit in II-VI semiconductors: The case of CdTe, Phys. Rev. B **66**, 155211 (2002).

[24] S.-H. Wei, Overcoming the doping bottleneck in semiconductors, Comput. Mater. Sci. **30**, 337 (2004).

[25] See Supplemental Materials at http://link.aps.org/supplemental/10.1103/PhysRevApplied.11.054058 for the stable chemical regions of $Ga_{1-x}Mn_xAs$ and $Ga_{1-x}Fe_xSb$, the electronic structure of III-V semiconductors doped with a single isolated Fe atom, and the crystal structure and band-coupling model of FDMSs.

[26] Y.-H. Li, A. Walsh, S. Chen, W.-J. Yin, J.-H. Yang, J. Li, J. L. F. Da Silva, X. G. Gong, and S.-H. Wei, Revised ab initio natural band offsets of all group IV, II-VI, and III-V semiconductors, Appl. Phys. Lett. **94**, 212109 (2009).

[27] M. Marsman, J. Paier, A. Stroppa, and G. Kresse, Hybrid functionals applied to extended systems, J. Phys.: Condens. Matter. **20**, 064201 (2008).

[28] H. Akai, Ferromagnetism and its Stability in the Diluted Magnetic Semiconductor (In, Mn) As, Phys. Rev. Lett. **81**, 3002 (1998).

[29] R. Colombelli, V. Piazza, A. Badolato, M. Lazzarino, F. Beltram, W. Schoenfeld, and P. Petroff, Conduction-band offset of single InAs monolayers on GaAs, Appl. Phys. Lett. **76**, 1146 (2000).

[30] O. Madelung, *Semiconductors: data handbook* (Springer Science & Business Media, 2012).

[31] L. Chen, S. Yan, P. F. Xu, J. Lu, W. Z. Wang, J. J. Deng, X. Qian, Y. Ji, and J. H. Zhao, Low-temperature magnetotransport behaviors of heavily Mn-doped (Ga, Mn)As films with high ferromagnetic transition temperature, Appl. Phys. Lett. **95**, 182505 (2009).

[32] D. Chiba, Y. Nishitani, F. Matsukura, and H. Ohno, Properties of $Ga_{1-x}Mn_xAs$ with high Mn composition ($x > 0.1$), Appl. Phys. Lett. **90**, 122503 (2007).

[33] S. Mack, R. C. Myers, J. T. Heron, A. C. Gossard, and D. D. Awschalom, Stoichiometric growth of high Curie temperature heavily alloyed GaMnAs, Appl. Phys. Lett. **92**, 192502 (2008).

[34] S. Ohya, K. Ohno, and M. Tanaka, Magneto-optical and magnetotransport properties of heavily Mn-doped GaMnAs, Appl. Phys. Lett. **90**, 112503 (2007).